Title

HIF-2α Preserves Mitochondrial Activity and Glucose Sensing in Compensating β-Cells in Obesity.

Journal

Diabetes, 71(7)

ISSN

0012-1797

Authors

Moon, Jae-Su
Riopel, Matthew
Seo, Jong Bae
et al.

Publication Date

2022-07-01

DOI

10.2337/db21-0736

Peer reviewed

HIF-2α Preserves Mitochondrial Activity and Glucose Sensing in Compensating β-Cells in Obesity

Jae-Su Moon,[1] Matthew Riopel,[1] Jong Bae Seo,[1] Vicente Herrero-Aguayo,[1,2] Roi Isaac,[1] and Yun Sok Lee[1]

Diabetes 2022;71:1508–1524 | https://doi.org/10.2337/db21-0736

In obesity, increased mitochondrial metabolism with the accumulation of oxidative stress leads to mitochondrial damage and β-cell dysfunction. In particular, β-cells express antioxidant enzymes at relatively low levels and are highly vulnerable to oxidative stress. Early in the development of obesity, β-cells exhibit increased glucose-stimulated insulin secretion in order to compensate for insulin resistance. This increase in β-cell function under the condition of enhanced metabolic stress suggests that β-cells possess a defense mechanism against increased oxidative damage, which may become insufficient or decline at the onset of type 2 diabetes. Here, we show that metabolic stress induces β-cell hypoxia inducible factor 2α (HIF-2α), which stimulates antioxidant gene expression (e.g., *Sod2* and *Cat*) and protects against mitochondrial reactive oxygen species (ROS) and subsequent mitochondrial damage. Knockdown of HIF-2α in Min6 cells exaggerated chronic high glucose–induced mitochondrial damage and β-cell dysfunction by increasing mitochondrial ROS levels. Moreover, inducible β-cell HIF-2α knockout mice developed more severe β-cell dysfunction and glucose intolerance on a high-fat diet, along with increased ROS levels and decreased islet mitochondrial mass. Our results provide a previously unknown mechanism through which β-cells defend against increased metabolic stress to promote β-cell compensation in obesity.

β-Cell dysfunction is a critical etiologic component of type 2 diabetes mellitus (T2DM) (1). During the development of obesity, β-cells respond to insulin resistance by adaptively increasing insulin secretion. However, with the onset of T2DM or impaired glucose tolerance, β-cell insulin secretion declines (2–4), with decreased β-cell mass and glucose-stimulated insulin secretion (GSIS) (5–8). Moreover, the incretin effect also declines in patients with T2DM, with increased hepatoporto GLP-1 inactivation, further limiting the postprandial increase in plasma insulin levels (9,10).

The intracellular mechanisms by which β-cell dysfunction develops in T2DM have been studied, and increased oxidative stress has been implicated as a causal mechanism (1,11,12). Mitochondrial metabolism is an essential component of β-cell glucose sensing and energy production, and this is accompanied by production of superoxide free radicals (13,14). In normal islets, glucose induces low levels of reactive oxygen species (ROS), which functions as a signal to enhance GSIS (15,16). However, in obesity, a chronic increase in mitochondrial metabolism enhances electron flux along the mitochondrial transport chain, resulting in premature electron escape to molecular oxygen (ROS production). This causes mitochondrial damage, leading to decreased GSIS and increased β-cell death (glucolipotoxicity) (1,17–21). In addition, accumulation of endoplasmic reticulum stress (22,23) and islet amyloid polypeptide (24) and inflammation (11,25) also stimulate cytosolic pro-oxidant enzyme expression/activity (e.g., NADPH oxidase and inducible nitric oxide synthase [iNOS]) (26,27). Indeed, oxidative stress is increased in T2DM islets and obese rodent islets (28–30), along with abnormal mitochondrial morphology and function (31,32). Moreover, treatment with chemical antioxidants (e.g., N-acetyl cysteine or aminoguanidine) improves β-cell function in obese rodents (32,33) or isolated islets exposed to chronic high glucose levels ex vivo (34).

In mammalian cells, superoxide free radicals are quickly converted to hydrogen peroxide by superoxide dismutases

[1]Division of Endocrinology and Metabolism, Department of Medicine, University of California San Diego, La Jolla, CA
[2]Maimonides Institute of Biomedical Research of Cordoba, Cordoba, Spain
Corresponding author: Yun Sok Lee, yunsoklee@ucsd.edu

Received 18 August 2021 and accepted 8 April 2022
J.B.S. is currently affiliated with Mokpo National University, Cheonggye-myeon, Republic of Korea.
This article contains supplementary material online at https://doi.org/10.2337/figshare.19607331.

(SODs) and then further metabolized into water by glutathione peroxidase (GPx) and catalase (35). However, in β-cells, the expression of these antioxidant enzymes is relatively low (0–40% of liver) (36,37), and therefore, β-cells are thought to be highly sensitive to oxidative stress. Consistent with this idea, overexpression of various antioxidant enzymes protects from the development of β-cell dysfunction. For example, among genetically obese and insulin resistant *db/db* mice, those engineered to overexpress GPx1 in β-cells are protected against the development of hyperglycemia (38). Moreover, overexpression of catalase, cytosolic Cu,Zn-SOD, or mitochondrial Mn-SOD protects against streptozotocin-induced β-cell loss in mice (39–42).

Tissue oxygen tension critically affects cell growth, metabolism, and function. Cellular responses to decreased oxygen tension (hypoxia) are largely mediated by hypoxia-inducible factors (HIFs) (43–45). The HIF is a heterodimeric transcription factor consisting of an oxygen-sensitive HIF-α subunit and a constitutively active HIF-1β (also known as aryl hydrocarbon receptor nuclear translocator 1 [Arnt1]) subunit. HIF-αs are ubiquitously expressed, but under normal oxygen concentration, they are rapidly degraded through a mechanism involving prolyl hydroxylase domain enzymes (PHDs) and von Hippel-Lindau (VHL) E3 ubiquitin ligase. In hypoxia, PHDs are inactivated, and stabilized HIF-αs translocate to the nucleus and induce genes necessary for adaptation to decreased oxygen levels. These include genes involved in anaerobic respiration (e.g., *Slc2a1* and *Pdk1*) and/or resistance to oxidative stress (e.g., *Gpx1, Cat*, *Fxn*, and *SOD*) (46). In humans and mice, three isoforms of the HIF-α subunit have been identified (HIF-1α, HIF-2α, and HIF-3α). Among these, HIF-1α and HIF-2α (also known as EPAS1) possess transactivation domains. Of interest, although HIF-1α and HIF-2α share 48% amino acid sequence identity with several common target genes, they mediate distinct physiologic effects. In β-cells, HIF-1α suppresses embryonic β-cell development, and dynamic suppression of HIF-1α expression in embryonic islets is required for islet development (47), whereas HIF-2α is necessary for embryonic pancreatic development in mice (48). HIF-1α also regulates the function of β-cells in adult mice. High levels of glucose or GLP-1 promote HIF-1α expression in β-cell lines (49,50). In T2DM, mRNA expression of *Arnt1*/*Hif1b* and *Hif1a* is decreased in islets compared with normal subjects, and β-cell–specific *Arnt1* or *Hif1a* knockout (KO) mice develop glucose intolerance as a result of decreased insulin secretion (51,52). These results suggest that physiologic HIF-1α expression is necessary to maintain normal β-cell function.

Although HIF-2α plays a crucial role in the regulation of oxygen and metabolic homeostasis, it is not yet known whether HIF-2α plays a role in the regulation of adult β-cell function, particularly during the pathogenesis of β-cell dysfunction in obesity and T2DM. In this article, we investigate the effect of HIF-2α in the regulation of β-cell insulin secretion in normal chow diet (NCD)–fed/lean and high-fat diet (HFD)–fed/obese mice, isolated primary islets, and Min6 cells.

RESEARCH DESIGN AND METHODS

Animals

To generate inducible β-cell–specific HIF-2α KO mice, $Hif2a^{fl/fl}$ mice were crossed with mice expressing Cre recombinase–mutated estrogen receptor fusion protein (Cre-ERT) under the control of the mouse insulin promoter (MIP-$CreERT^{+/-}$:$Hif2a^{fl/fl}$, $H2\beta KO^{MIP}$) (53) or the pancreatic and duodenal homeobox 1 (*Pdx*1) promoter (*Pdx1-*$CreERT^{+/-}$:$Hif2a^{fl/fl}$, $H2\beta KO^{PDX1}$) (54). Mice were housed in colony cages in 12 h light/12 h dark cycles. For the HFD study, male mice were subjected to 60% HFD (cat. no. D12492; Research Diets, Inc.). After 12 weeks of this HFD, the diet was switched to a tamoxifen-containing HFD for 1 week to induce Cre activation and then switched back to the regular HFD not containing tamoxifen until the termination of the experiments. After 2 weeks of recovery and tamoxifen clearance, mice underwent oral glucose tolerance tests. Briefly, the mice were fasted for 6 h, and basal blood samples were taken, followed by oral glucose gavage (2 g/kg). Blood samples were drawn at 10, 20, 30, 45, 60, 90, and 120 min after gavage, as described previously (55,56). Phenotypes of $H2\beta KO^{MIP}$ or $H2\beta KO^{PDX1}$ mice were compared with those of $Cre^{-/-}$ littermate control mice ($Cre^{-/-}$:$Hif2a^{fl/fl}$) and/or age-matched MIP-$CreERT^{+}$:$Hif2a^{+/+}$ mice (MIP-CreERT). To avoid possible experimental bias resulting from the use of tamoxifen (57), all mice, including $Cre^{-/-}$ control mice, were given tamoxifen before analyses. All animal procedures were performed in accordance with an Institutional Animal Care and Use Committee–approved protocol and the research guidelines for the use of laboratory animals of the University of California San Diego.

Histology

Immunohistochemistry (IHC) and β-cell mass analyses were performed as described previously (58). Briefly, deparaffinized tissue sections were washed with once with Tris-buffered saline with Tween 20 (TBST) and blocked for endogenous peroxidase and background staining by 10-min incubation in Ultravision Hydrogen Peroxidase Block (Thermo Fisher Scientific) solution, followed by another 10 min incubation in Background Punisher (cat. no. BP974M; BioCare). Each step of blocking was followed by an interval in which the slides were washed twice in TBST. Sections were then incubated with control immunoglobulin G (IgG), anti-insulin (cat. no. A0564; Dako), and/or antiglucagon (cat. no. PA1-85465; Pierce Biotechnology, Inc.) antibodies, followed by incubation with secondary antibodies conjugated with horseradish peroxidase (cat. no. 711-036-152; Jackson ImmunoResearch Laboratories) for 30 min. After washing with TBST twice, DAB chromogens (cat. no. 95041-478; VWR) were applied for 5 min and washed

twice in double-distilled water, followed by Mayer's hematoxylin counterstaining for 5 min. For morphometry analyses, images were captured using a NanoZoomer slide scanner system with NanoZoomer Digital Pathology software (Hamamatsu Photonics) and analyzed using ImageJ software (National Institutes of Health, Bethesda, MD). For HIF-2α IHC studies, whole pancreata were excised and snap frozen at an optimum cutting temperature (Fisher Healthcare). Tissue sections measuring 5 μm were fixed with 4% paraformaldehyde for 15 min at room temperature and were subsequently incubated in hydrogen peroxide for 10 min at room temperature for quenching of endogenous peroxidases. Before adding primary antibodies, sections were blocked with 1% bovine serum albumin (BSA) for 30 min at room temperature. Fixed tissue sections were incubated with primary antibodies (guinea pig anti-human insulin [cat. no. IS002; Dako] and rabbit anti–HIF-2α [cat. no. NB100-122; Novus]) (dilution of 1:200), followed by incubation with secondary antibodies. For detecting insulin, anti-rabbit IgG (goat) conjugated with biotin (cat. no. NEF813001EA; Jackson ImmunoResearch Laboratories) and streptavidin conjugated with Alexa Fluor 647 (cat. no. 016-600-084; Jackson ImmunoResearch Laboratories) were used. For detecting HIF-2α, the PerkinElmer TSA Fluorescein Kit (cat. no. NEL701A001KT) was used. Nuclei were stained with DAPI. Images were acquired on a Leica SP8 confocal microscope and processed with ImageJ software.

Plasma Insulin and C-Peptide Concentration and Intraislet Insulin Content

Plasma insulin (cat. no. 80-INSHU-E01.1; Alpco Diagnostics) and C-peptide (cat. no. CPTHUE01.1; Alpco Diagnostics) levels were measured by ELISA in accordance with the manufacturers' instructions. Pancreatic insulin content was determined as described previously (58).

Quantitative Real-Time PCR

Total RNA was extracted by TRIzol reagent (cat. no. 15596026; Invitrogen) or RNeasy Mini Kit (cat. no. 74104; QIAGEN). Synthesis of cDNA was performed using the High-Capacity cDNA Reverse Transcription Kit (cat. no. 4368813; Applied Biosystems). Quantitative real-time PCR was performed using Power SYBR Green PCR Master Mix (cat. no. 4312704; Thermo Fisher Scientific). Primer sequences are shown in Supplementary Table 1.

Western Blot Analysis

Tissues and cells were lysed in lysis buffer (20 mmol/L Tris-HCl [pH 7.4], 100 mmol/L NaCl, 1.5 mmol/L $MgCl_2$, and 0.1% [vol/vol] Nonidet P-40) containing protease and phosphatase inhibitor cocktail (cat. nos. 04693159001 and 04906845001, respectively; Roche Diagnostics) and then centrifuged at 13,000 rpm for 15 min at 4°C. The supernatants were separated in SDS-PAGE gels (cat. no. 567-1084; Bio-Rad Laboratories) and electrotransferred to polyvinylidene difluoride membranes. The membranes were blocked for 1 h in TBST (10 mmol/L Tris-HCl and 0.1% TritonX-100 [pH 7.4]) containing 5% BSA and then incubated with specific antibodies at 4°C overnight: HIF-1α (cat. no. ab-2185; Abcam), HIF-2α (cat. no. NB100-122; Novus Biologicals), and actin (cat. no. A2228; Sigma). After washing with fresh TBST, the membrane was incubated with secondary antibody conjugated with horseradish peroxidase specific to rabbit or mouse IgG (Jackson ImmunoResearch Laboratories) (dilution of 1:5,000) and visualized using the ECL system (cat. no. WBKLS0050; Merck Millipore) followed by autoradiography or the Bio-Rad ChemiDoc XRS$^+$ imaging system. Intensity of the bands in the autoradiograms was measured using ImageJ software.

HIF-2α Knockdown and GSIS Assay

For HIF-2α knockdown (KD) studies, Min6 cells (passage numbers of ∼12–15) were transfected with mock or *Hif2a*-specific siRNAs using lipofectamine RNA iMAX reagent (cat. no. 11668030; Invitrogen). Six hours after transfection, media were changed to appropriate media in accordance with each of the experimental conditions. *Hif2a*-specific siRNA was purchased from Dharmacon (cat. no. L-040635-01-005; ON-TARGETplus siRNA). Static GSIS assays were performed as described previously (58). Briefly, Min6 cells were incubated in 2.8 mmol/L glucose DMEM for 5 h and washed twice with Krebs-Ringer bicarbonate buffer (KRBB) (2.5 mmol/L CaCl2/2H2O, 1.16 mmol/L MgSO4/7H2O, 1.2 mmol/L KH2PO4, 4.7 mmol/L KCl, 114 mmol/L NaCl, 25.5 mmol/L NaHCO3, 20 mmol/L HEPES/Na-HEPES, and 0.2% BSA). Basal insulin release was measured after incubating the cells in KRBB supplemented by 2.8 mmol/L glucose for 30 min. Glucose-stimulated insulin secretion was measured after incubating the cells in KRBB supplemented by 16.7 mmol/L glucose for 30 min.

Citrate Synthase Activity

Citrate synthase (CS) activity was measured using a commercial kit according to the manufacturer's instructions (cat. no. K318-100; BioVision).

Immunofluorescence Analysis of Mitochondrial Density

A total of 50,000 Min6 cells were seeded in each well of the four-chamber plate (cat. no. 08-774-215; Corning) and grown in DMEM (5 g/L glucose, 4% v/v fetal bovine serum, and 0.1% v/v penicillin/streptomycin) for 24 h. Cells were transfected with 20 nmol/L control or *Hif2a*-specific siRNA using Lipofectamin RNA iMAX (cat. no. 11668030; Invitrogen). Six hours after transfection, media were changed with fresh media. Media were changed with fresh 2.8 or 16.8 mmol/L glucose media 24 h after transfection. After 24 h, cells were fixed with 4% paraformaldehyde and permeabilized with 0.2% Triton X-100 and 1% BSA phosphate-buffered saline (PBS), followed by blocking

with 1% BSA PBS. To stain with anti-Tom20 antibody, cells were incubated with anti-Tom20 antibody (cat. no. sc-17764; Santa Cruz Biotechnology) (dilution of 1:500) overnight at 4°C, followed by incubation with secondary antibodies conjugated with Alexa Fluor 488 (cat. no. A32723; Invitrogen) (dilution of 1:200) for 1 h at room temperature. Nuclei were stained with DAPI (cat. no. ab228549; Abcam). Images were acquired on a Leica SP8 confocal microscope and were processed with ImageJ software.

Intracellular Lactate Concentration

Lactate content in total lysate of Min6 cells was measured by using the Lactate Colorimetric Assay Kit (cat. no. K607-100; BioVision, Inc., Milpitas, CA).

Glucose Uptake

Min6 cells were seeded at 100,000 cells per 24-well plate and grown in DMEM containing 5 g/L glucose, 4% v/v FBS, and 0.1% v/v penicillin/streptomycin. The cells were washed with fresh 2.8 mmol/L glucose KRBB (2.6 mmol/L CaCl2/2H2O, 1.2 mmol/L MgSO4/7H2O, 1.2 mmol/L KH2PO4, 4.9 mmol/L KCl, 98.5 mmol/L NaCl, and 25.9 mmol/L NaHCO3, supplemented with 20 mmol/L HEPES and 0.1% BSA) (cat. no. A8806; Sigma). After incubating with 2.8 mmol/L glucose KRBB for 5 h, the cells were incubated with 2.8 and 16.8 mmol/L glucose KRBB for 1 h with 2-deoxyglucose labeled with tritium (2.8 mmol/L cold glucose with 0.16 μCi/mL [^{3}H]glucose and 16.8 mmol/L cold glucose with 1 μCi/mL of [^{3}H]glucose). After three washings in ice-cold PBS, the cells were lysed in lysis buffer with 0.1% sodium dodecyl sulfate and subjected to scintillation counting to determine their ^{3}H radioactivity, and radioactivity was normalized by total protein content.

Measurement of Intracellular and Mitochondrial ROS

Cytosolic and mitochondrial ROS levels were measured using 5- and 6-chloromethyl-2′, 7′-dichlorodihydro-fluorescein diacetate (cat. no. C6827; Thermo Fisher Scientific) and MitoSOX red (cat. no. M36008; Thermo Fisher Scientific) fluorescent dyes, respectively. Thirty minutes after dye loading, fluorescence intensity in each of the wells was measured using a multiplate reader (FilterMax F5; Molecular Devices).

Isolation of Primary Mouse Islets

Primary mouse islet isolation was performed as described previously with minor modifications (58). Briefly, the bile duct near the ampulla of Vater was ligated, and the common bile duct was cannulated and injected with 3 mL KRBB containing collagenase XI (800 U/mL) (Sigma, Ronkonkoma, NY). The pancreas was dissected from the surrounding tissues, removed, and incubated in a stationary bath for 15 min at 37°C. The digested tissue was washed with KRB without collagenase, and the islets were then purified by a density gradient (Histopaque 1077 and 1119; Sigma) centrifuged at 3,000*g* for 25 min. Collagen-digested pancreata were filtered through 1,000- and 500-μm sieves, and islets >75 and <250 μm were handpicked under a stereoscope. Islets were cultured in suspension in RPMI 1640 medium, 5 mmol/L glucose, 10% fetal calf serum, 50 units/mL penicillin, 50 μg/mL streptomycin, and 40 μg/mL gentamicin. For Western blots, islets (~150–200 per well) were kept under normoxic or hypoxic conditions (1% O_2) for 6 h. RIPA lysis buffer (25 mmol/L Tris-Cl [pH 7.4], 150 mmol/L NaCl, 1% NP-40, 0.5% sodium deoxycholate, 0.1% SDS, protease inhibitor, and phosphatase inhibitor) was added within the hypoxia chamber, and cells were lysed.

Mitochondrial DNA Content

Total DNA was extracted from cells by the proteinase K DNA extraction method. The relative mitochondrial DNA copy number was determined by normalizing mitochondrial DNA copy number to nuclear DNA (18S rRNA) copy number. Primer sequences are shown in Supplementary Table 1.

Intracellular Nitrite Level

Intracellular nitrite content was measured using the Griess Reagent System (cat. no. G2930; Promega) in accordance with the manufacturer's protocol.

Data and Resource Availability

The data generated during this study are available upon reasonable request. Resources generated during this study are available upon reasonable request.

RESULTS

Obesity Induces β-Cell HIF-2α Expression

In mice, HFD-induced β-cell dysfunction involves progressive deterioration of GSIS, along with increased islet mass and basal insulin secretion, compared with NCD (59,60). To understand whether β-cell HIF-2α expression is changed in obesity, we measured mRNA expression of *Hif2a* in islets from NCD- and HFD-fed mice. Going from NCD to HFD, *Hif1a* mRNA expression was moderately increased, whereas the enhanced expression of *Hif2a* was more robust (Fig. 1*A*). Because HIF-2α is regulated by posttranslational regulation of protein stability, we assessed β-cell HIF-2α protein expression in NCD- and HFD-fed mice after fasting and refeeding. Hyperoxia and cellular stress during islet isolation can profoundly affect HIF-2α expression; therefore, we chose IHC analysis in snap-frozen pancreatic tissue sections processed and stained side by side and imaged under the same microscopic settings. As seen in Fig. 1*B* and *C*, in β-cells from fasted NCD-fed mice, HIF-2α expression was relatively low, and the majority of HIF-2α was located in the cytoplasm. Upon refeeding, the majority of HIF-2α was translocated to the nucleus, without changes in overall HIF-2α expression (Fig. 1*B* and *C*). In HFD-fed/obese mice, overall β-cell HIF-2α

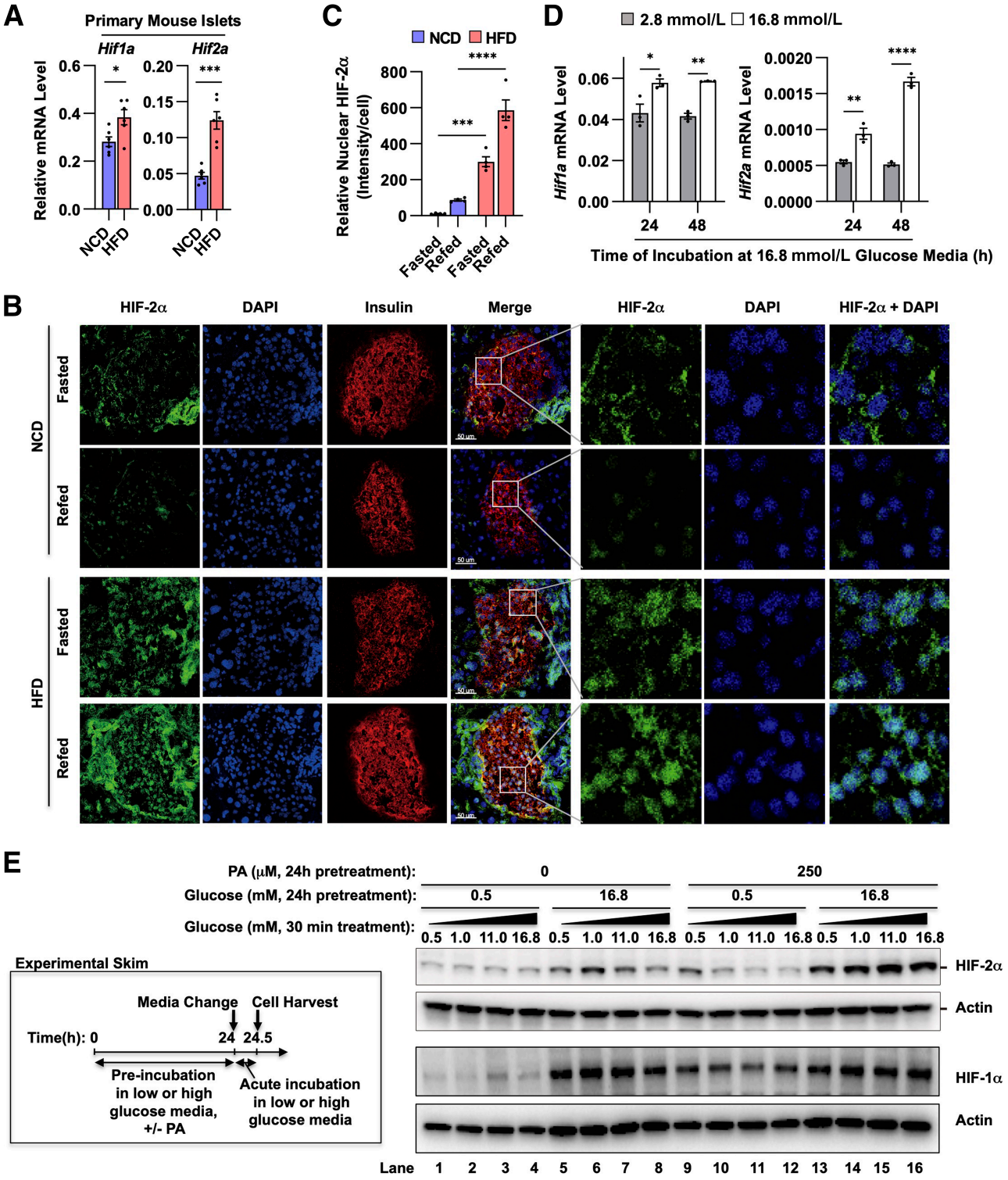

Figure 1—Metabolic stress increases β-cell HIF-2α expression. *A*: mRNA expression of *Hif1a* and *Epas1*/*Hif2a* in primary islets from NCD- and HFD-fed mice ($n = 6$ mice per group). *B*: IHC analysis of HIF-2α expression in pancreatic islets of NCD-fed and 12-week HFD-fed mice. *C*: Densitometric analysis of nuclear HIF-2α expression (HIF-2α expression in DAPI-positive area) in the images in panel *B*. *D*: mRNA expression of *Hif1a* and *Epas1*/*Hif2a* in Min6 cells incubated in low- (2.8 mmol/L) and high-glucose (16.8 mmol/L) conditions for 24 or 48 h ($n = 3$ wells per group). *E*: Western blot analysis of HIF-1α and HIF-2α expression in Min6 cells. Cells were preincubated in low- (0.5 mmol/L) or high-glucose (16.8 mmol/L) media, with or without 250 μmol/L PA for 24 h, followed by 30-min incubation in 0.5–16.8 mmol/L glucose media, as illustrated in the box on left. *$P < 0.05$, **$P < 0.01$, ***$P < 0.001$, ****$P < 0.0001$ versus lane 1. All data are presented as mean ± SEM. Statistical analysis was performed by unpaired *t* test (*A*) or two-way ANOVA with Tukey multiple comparison tests (*C* and *D*).

expression was markedly increased compared with lean mice, and the majority of HIF-2α was observed in the nucleus regardless of feeding state (Fig. 1*B* and *C* and Supplementary Fig. 1*A*). To test whether HFD-induced β-cell *Hif2a* mRNA and protein expression result from increased metabolic stress, we incubated Min6 cells in high-glucose (16.8 mmol/L) media for 24 and 48 h and measured *Hif2a* expression. Unlike islets, baseline *Hif2a* expression was lower compared with *Hif1a* in Min6 cells (Fig. 1*D*). Nonetheless, after chronic incubation in high-glucose media, mRNA expression of *Hif1a* was somewhat increased (∼37%), whereas the increase in *Hif2a* mRNA expression was considerably greater (∼200%). Moreover, HIF-2α protein expression was markedly increased after 24-h incubation in high-glucose media, which was enhanced by cotreatment with palmitic acid (PA) (Fig. 1*E* and Supplementary Fig. 1*B*). HIF-2α expression remained unchanged after acute (30 min) high-glucose challenge (Fig. 1*E* and Supplementary Fig. 1*B*). HIF-1α expression was also increased by both acute and chronic high-glucose challenges, and PA treatment increased HIF-1α expression in both low- and high-glucose conditions (Fig. 1*E* and Supplementary Fig. 1*B*). These changes in HIF-α expression were associated with decreased intracellular oxygen levels (hypoxia) as measured by pimonidazole adduct formation (Supplementary Fig. 1*C* and *D*). Together, these results suggest that chronic metabolic stress in obese β-cells promotes HIF-2α expression.

Generation of Inducible β-Cell–Specific HIF-2α KO Mice

To assess the effect of HIF-2α on β-cell growth and function, we generated β-cell–specific HIF-2α KO mice. Because conventional HIF-2α KO mice develop defective pancreatic development (48), to assess the effect of HIF-2α on adult β-cell function, we generated inducible β-cell–specific HIF-2α KO (H2βKO) mice using the Cre-LoxP system. Specifically, we generated two different inducible H2βKO strains using MIP-CreERT ($H2\beta KO^{MIP}$) (53) and *Pdx1*-CreERT ($H2\beta KO^{PDX1}$) (54) mice. To induce Cre activity, mice were fed chow containing tamoxifen for 1 week. After 2 weeks of recovery, mice were subjected to oral glucose tolerance tests as illustrated in Supplementary Fig. 2*A*. When assessed 3 weeks after final tamoxifen administration, *Hif2a* mRNA and HIF-2α protein expression were decreased by 67–87% in the primary islets from $H2\beta KO^{MIP}$ or $H2\beta KO^{PDX1}$ mice compared with $CreERT^{-/-}$:$Hif2a^{fl/fl}$ littermate or age-matched MIP-CreERT control mice, without changes in *Hif1a* or HIF-1α expression (Supplementary Fig. 2*B–D*). Body weight remained comparable between $H2\beta KO^{MIP}$, $Cre^{-/-}$:$Hif2a^{fl/fl}$, and MIP-CreERT mice or between $H2\beta KO^{PDX1}$ and $Cre^{-/-}$:$Hif2a^{fl/fl}$ mice before (data not shown) and after tamoxifen treatment (Supplementary Fig. 2*E* and *F*).

Inducible Depletion of β-Cell HIF-2α Does Not Impair Glucose Tolerance in Mice Fed NCD

Fasting blood glucose levels and glucose tolerance were comparable in $H2\beta KO^{MIP}$ and $H2\beta KO^{PDX1}$ mice compared with $Cre^{-/-}$:$Hif2a^{fl/fl}$ and/or MIP-CreERT mice on NCD, with comparable levels of plasma insulin and C-peptide (Supplementary Fig. 2*G–J*). Moreover, the characteristic features of islet morphology, such as predominance of insulin-positive β-cells in the core mantled by glucagon-positive α-cells, were unchanged in NCD-fed $H2\beta KO^{MIP}$ and $H2\beta KO^{PDX1}$ mice compared with NCD $Cre^{-/-}$:$Hif2a^{fl/fl}$ or MIP-CreERT mice (Supplementary Fig. 2*K* and *L*). Although β-cell mass was slightly increased in $H2\beta KO^{MIP}$ mice, with a tendency toward increased islet number (Supplementary Fig. 2*M* and *N*), β-cell mass and islet number were unchanged in $H2\beta KO^{PDX1}$ mice compared with $Cre^{-/-}$:$Hif2a^{fl/fl}$ mice (Supplementary Fig. 2*O* and *P*). Moreover, pancreatic mass was unchanged in the two H2βKO mouse strains (Supplementary Fig. 2*Q* and *R*). Interestingly, although glucose tolerance was unchanged, ex vivo GSIS was slightly decreased in the islets from $H2\beta KO^{MIP}$ and $H2\beta KO^{PDX}$ mice compared with the islets from $Cre^{-/-}$:$Hif2a^{fl/fl}$ and MIP-CreERT mice (Supplementary Fig. 2*S*).

β-Cell HIF-2α Depletion Impairs GSIS and Worsens Obesity-Induced Glucose Intolerance

Because β-cell HIF-2α expression was increased in HFD-fed mice, we assessed the effect of β-cell HIF-2α KO in HFD-fed/obese mice. $H2\beta KO^{MIP}$, $H2\beta KO^{PDX1}$, and wild-type (WT) littermate control mice ($Cre^{-/-}$:$Hif2a^{fl/fl}$) and age-matched MIP-CreERT mice were fed an HFD and treated with tamoxifen as illustrated in Fig. 2*A*. After tamoxifen treatment, body weight remain comparable between $Cre^{-/-}$:$Hif2a^{fl/fl}$, MIP-CreERT, and $H2\beta KO^{MIP}$ mice and between $Cre^{-/-}$:$Hif2a^{fl/fl}$ and $H2\beta KO^{PDX1}$ mice (Fig. 2*B* and *C* and Supplementary Fig. 3*A*). Interestingly, HFD-fed $H2\beta KO^{PDX1}$ mice showed impaired glucose tolerance compared with HFD-fed $Cre^{-/-}$:$Hif2a^{fl/fl}$ littermate control mice (Fig. 2*D* and Supplementary Fig. 3*B*). Consistent with this, glucose tolerance was worse in HFD-fed $H2\beta KO^{MIP}$ mice compared with HFD-fed $Cre^{-/-}$:$Hif2a^{fl/fl}$ and MIP-CreERT control mice (Fig. 2*E*). This change was associated with decreased plasma insulin and C-peptide levels after glucose challenge in fasted HFD-fed $H2\beta KO^{MIP}$ mice compared with fasted HFD-fed $Cre^{-/-}$:$Hif2a^{fl/fl}$ and HFD-fed MIP-CreERT mice (Fig. 2*F* and *G*). Moreover, ex vivo GSIS was markedly decreased in isolated islets from HFD-fed $H2\beta KO^{MIP}$ and $H2\beta KO^{PDX1}$ mice compared with the islets from HFD-fed $Cre^{-/-}$:$Hif2a^{fl/fl}$ littermate and/or MIP-CreERT control mice (Fig. 2*H*). Intracellular insulin content per islet was not decreased in KO islets (Supplementary Fig. 3*C*). Furthermore, glucose plus GLP-1–stimulated insulin secretion was lower in the islets from HFD-fed $H2\beta KO^{MIP}$ mice compared with HFD-fed MIP-CreERT mice (Supplementary Fig. 3*D*), suggesting that β-cell HIF-2α depletion exaggerates HFD/obesity-induced β-cell dysfunction. These changes

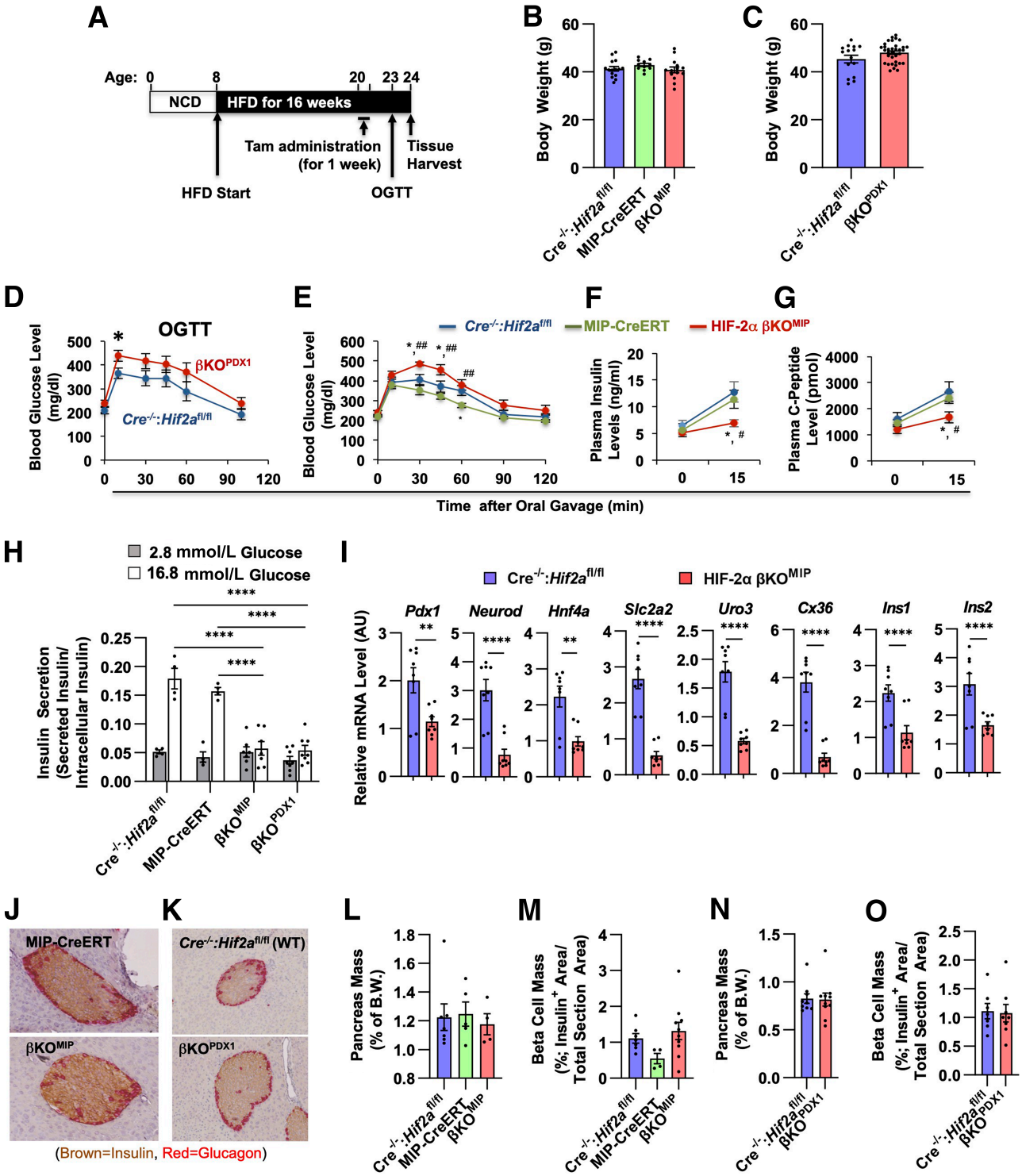

Figure 2—Inducible depletion of β-cell HIF-2α after onset of obesity and glucose intolerance worsens GSIS and glucose intolerance in mice. H2βKO^{MIP}, H2βKO^{PDX1}, Cre$^{-/-}$:*Hif2a*$^{fl/fl}$ littermate control, and age-matched MIP-CreERT mice were fed 60% HFD for 12 weeks, followed by 1 week of tamoxifen-containing HFD. After 2 weeks of recovery, mice underwent oral glucose tolerance tests (OGTTs). *A*: Schematic representation of experimental timeline. *B* and *C*: Body weight (BW) on the day of OGTT in panels *D* and *E* (n = 15, 11, and 14 mice per group in panel *B* and n = 15 and 35 mice per group in panel *C*). *D* and *E*: OGTTs (n = 9 and 10 mice in panel *D* and n = 11, 9, and 7 mice in panel *E*). *F*: Plasma insulin levels during OGTTs in panel *E* mice. *G*: Plasma C-peptide levels during OGTTs in panel *E* mice. *H*: Ex vivo static GSIS tests in isolated islets (n = 4, 4, 7, and 8 mice per group). *I*: mRNA expression of genes associated with β-cell function (n = 8 mice per group). *J–O*: Islet morphology analysis in HFD-fed MIP-CreERT and H2βKO^{MIP} (*J*) and *Cre*$^{-/-}$:*Hif2a*$^{fl/fl}$ and H2βKO^{PDX1} (*K*) mouse pancreatic sections after staining with anti-insulin and antiglucagon antibodies (n = 4 MIP-CreERT, 4 H2βKO^{MIP}, 5 *Cre*$^{-/-}$:*Hif2a*$^{fl/fl}$, and 4 H2βKO^{PDX1} mice were used for the analysis; representative figures are shown in panels *J* and *K*). *L* and *N*: Relative pancreatic mass (n = 7 *Cre*$^{-/-}$:*Hif2a*$^{fl/fl}$, 4 MIP-CreERT, and 5 H2βKO^{MIP} in panel *L* and 9 *Cre*$^{-/-}$:*Hif2a*$^{fl/fl}$ and 10 H2βKO^{PDX1} mice in panel *N*). *M* and *O*:

were associated with decreased expression of genes associated with β-cell differentiation, maturation, and function, such as *Pdx1*, *Neurod*, *Hnf4a*, *Slc2a2*, *Ins1*, *Ins2*, *Uro3*, and *Cx36*, in HFD-fed H2βKO^{MIP} mice compared with HFD-fed Cre$^{-/-}$:*Hif2a*$^{fl/fl}$ mice (Fig. 2*I*). Islet morphology was unchanged in the two H2βKO mouse strains compared with Cre$^{-/-}$:*Hif2a*$^{fl/fl}$ and MIP-CreERT control mice on HFD (Fig. 2*J* and *K*). Moreover, pancreatic mass, relative β-cell mass, and number of islets per section area were not decreased in HFD-fed H2βKO^{MIP} or H2βKO^{PDX1} mice compared with HFD-fed Cre$^{-/-}$:*Hif2a*$^{fl/fl}$ littermate control mice and/or age-matched MIP-CreERT mice (Fig. 2*L–O* and Supplementary Fig. 3*E* and *F*), suggesting that HIF-2α depletion impairs GSIS without affecting β-cell number or mass. Moreover, the proportion of α-cells and the ratio of α-cells/β-cells within each of the islets were unchanged in both HFD-fed H2βKO^{MIP} and H2βKO^{PDX1} mice compared with HFD-fed WT control mice (Supplementary Fig. 3*G–I*). Taken together, these results suggest that inducible β-cell HIF-2α depletion exacerbates obesity-induced impaired GSIS and glucose tolerance without affecting β-cell number or mass or the ratio of α-cells/β-cells.

HIF-2α KD Exacerbates Chronic High Glucose–Induced Impaired GSIS

To understand the mechanism through which HIF-2α regulates β-cell GSIS, we performed HIF-2α KD experiments in Min6 cells. Because β-cell HIF-2α expression was increased by chronic high glucose levels, we determined the effect of HIF-2α on β-cell function after chronic incubation in high- or low-glucose media as illustrated in Fig. 3*A*. To achieve HIF-2α KD, Min6 cells were transfected with mock or *Hif2a*-specifc siRNAs, followed by 24- or 48-h incubation in low- or high-glucose media. *Hif2a*-specific siRNA transfection reduced *Hif2a* and HIF-2α expression by >80% (Fig. 3*B* and *C*) and did not affect *Hif1a* or HIF-1α expression (Fig. 3*B* and *C* and Supplementary Fig. 4*A–C*). HIF-2α depletion can increase the number of free Arnt proteins that can heterodimerize with HIF-1α and thus indirectly enhance HIF-1α target gene expression. We also tested this hypothesis. When assessed by immunoprecipitation (with anti-Arnt antibodies)/Western blot analyses, Arnt-associated HIF-1α levels were not increased by HIF-2α KD (Supplementary Fig. 4*D*). Interestingly, chronic incubation in high-glucose media increased Arnt expression (along with HIF-1α and HIF-2α) (Supplementary Fig. 4*D*), suggesting that increased HIF-α protein levels are backed up by increased Arnt expression under metabolic stress. Taken together, these results suggest that high glucose–induced HIF-2α does not affect HIF-1α expression or limit free Arnt levels to heterodimerize with HIF-1α.

When measured under static incubation conditions, GSIS was decreased after chronic (24 or 48 h) preincubation in high-glucose media in mock siRNA–transfected control cells (Fig. 3*D*, lane 3 vs. 7), which is a widely recognized phenomenon known as glucotoxicity (61–63). Interestingly, HIF-2α KD exacerbated the decrease in GSIS induced by chronic preincubation in high-glucose media (Fig. 3*D*, lane 7 vs. 8). In contrast, HIF-2α KD did not affect GSIS in cells maintained in low-glucose media (Fig. 3*D*, lane 3 vs. 4), consistent with a previous report (49).

HIF-2α KD Enhances Metabolic Stress–Induced Mitochondrial Dysfunction

The process of GSIS is initiated by increased glucose uptake followed by increased mitochondrial metabolism, with an increase in the ATP/ADP ratio. This inhibits ATP-dependent potassium channel activity, leading to membrane depolarization, activation of voltage-dependent calcium channel, and increased intracellular calcium ion (Ca^{2+}) levels. Increased intracellular Ca^{2+} levels trigger insulin secretion. Therefore, we assessed whether HIF-2α KD lowers glucose-induced intracellular ATP levels after preincubation in low- or high-glucose media. In mock-transfected cells incubated in low-glucose media, intracellular ATP levels were induced by acute (30 min) high-glucose challenge (Fig. 4*A*, lane 1 vs. 3). Chronic preincubation in high-glucose media lowered the effect on acute high glucose–induced ATP levels (Fig. 4*A*, lane 3 vs. 7). This effect of preincubation in high-glucose media was associated with increased expression of *Pdk1* (Fig. 4*B*), which blocks mitochondrial pyruvate utilization. Moreover, preincubation in high-glucose media decreased intact mitochondrial mass as measured by CS activity (Fig. 4C). Consistently, immunocytochemical analysis of Tom20-positive mitochondrial mass revealed that HIF-2α KD enhanced chronic high glucose–induced decreased mitochondrial content (Fig. 4*D*). The expression of glucose transporters, including *Slc2a1* (encoding a high-affinity glucose transporter, Glut1) and *Slc2a2* (encoding the low-affinity high-capacity glucose transporter, Glut2), was slightly increased by chronic preincubation in high-glucose media (Fig. 4B); however, this did not lead to increased glucose uptake (Fig. 4*E*, lane 1 vs. 5 and lane 3 vs. 7). Intracellular lactate levels were higher in cells preincubated in high-glucose media for 48 h compared with cells maintained in low-glucose media (Fig. 4*F*). These results are consistent with the view that chronic high glucose levels impair GSIS by blocking mitochondrial metabolism (17). Interestingly,

Relative β mass was calculated by dividing insulin-positive area by total section area (n = 7 Cre$^{-/-}$:*Hif2a*$^{fl/fl}$, 4 MIP-CreERT, and 10 H2βKO^{MIP} mice in panel *M* and 7 Cre$^{-/-}$:*Hif2a*$^{fl/fl}$ and 8 H2βKO^{PDX1} mice in panel *O*). *P < 0.05, **P < 0.01, ****P < 0.0001 versus Cre$^{-/-}$:*Hif2a*$^{fl/fl}$ mice and $^{\#}P$ < 0.05, $^{\#\#}P$ < 0.01 versus MIP-CreERT mice, unless otherwise indicated. All data are presented as mean ± SEM. Statistical analysis was performed by one- (*I*) or two-way (*D–H*) ANOVA with Tukey multiple comparison tests. AU, arbitrary unit.

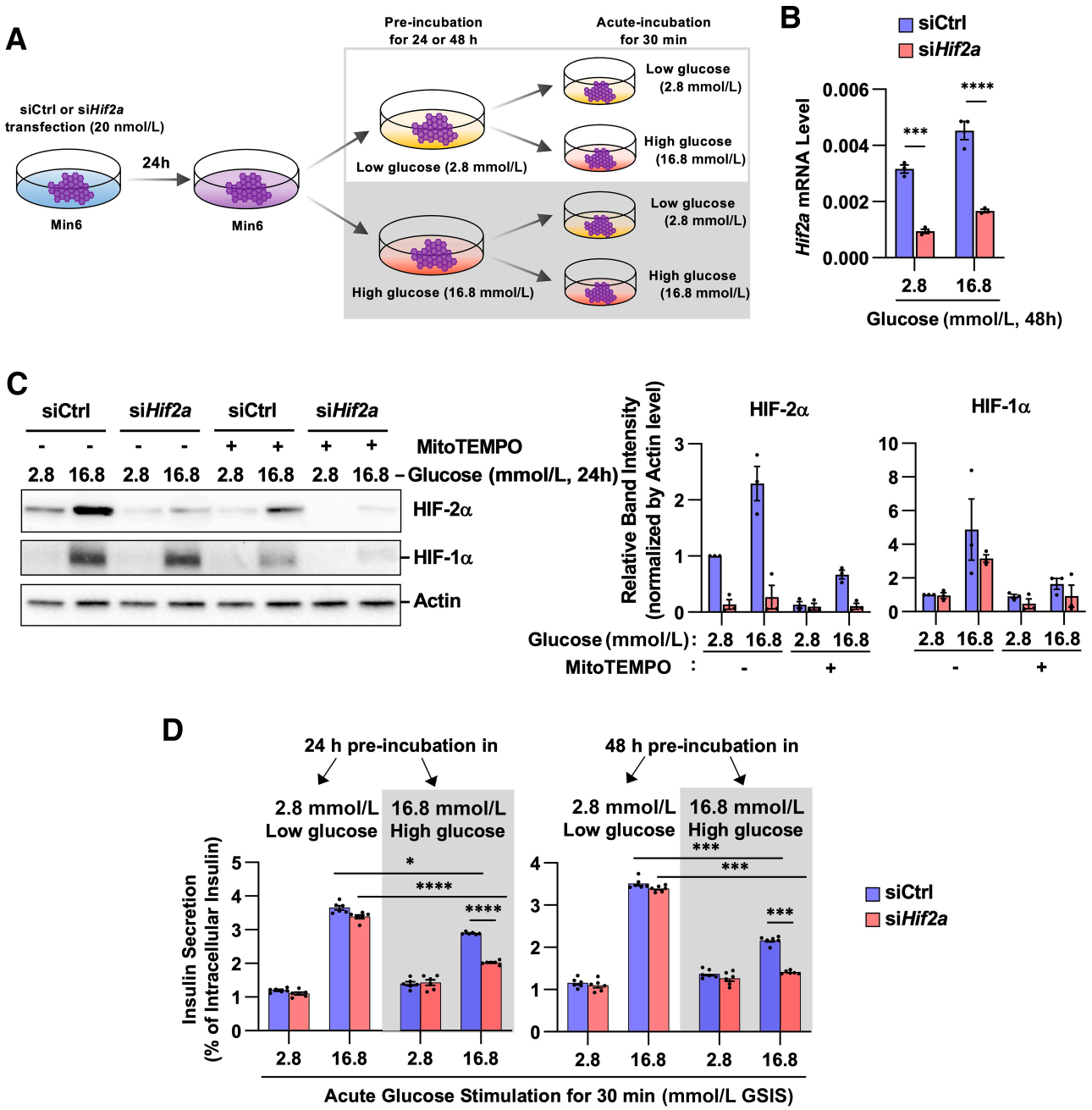

Figure 3—HIF-2α KD sensitizes β-cells to chronic high glucose–induced impaired GSIS in Min6 cells. Min6 cells were transfected with mock or *Hif2a*-specific siRNA; 24 h after transfection, cells were incubated in low- (2.8 mmol/L) or high-glucose (16.8 mmol/L) media for 24 or 48 h. *A*: Schematic representation of experimental skim. *B*: mRNA expression of *Hif2a* ($n = 3$ wells per group). *C*: Western blot analysis of HIF-1α and HIF-2α expression. Relative changes in HIF-1α and HIF-2α expression are plotted and presented on the right ($n = 3$ independent experiments). *D*: Static GSIS tests ($n = 6$ wells per group). $^*P < 0.05$, $^{***}P < 0.001$, $^{****}P < 0.0001$. All data are presented as mean ± SEM. Statistical analysis was performed by two-way ANOVA with Tukey multiple comparison tests.

HIF-2α KD exaggerated the decrease in glucose-stimulated intracellular ATP levels, conferred by chronic preincubation in high-glucose media (Fig. 4*A*, lane 7 vs. 8). These changes were associated with decreased intact mitochondrial mass (Fig. 4*C* and *D*). In contrast, the expression of glycolytic genes, such as *Slc2a1*, *Pdk1*, *Pgk1*, and *Ldha*, was not increased by HIF-2α KD in Min6 cells incubated in high-glucose media (Fig. 4*B*). Moreover, glucose uptake (Fig. 4*E*, lane 7 vs. 8) was not changed by HIF-2α KD, although *Slc2a2* expression was slightly decreased (Fig. 4*B*). Taken together, these results suggest that HIF-2α KD exacerbates chronic high glucose–induced impaired GSIS by enhancing mitochondrial dysfunction.

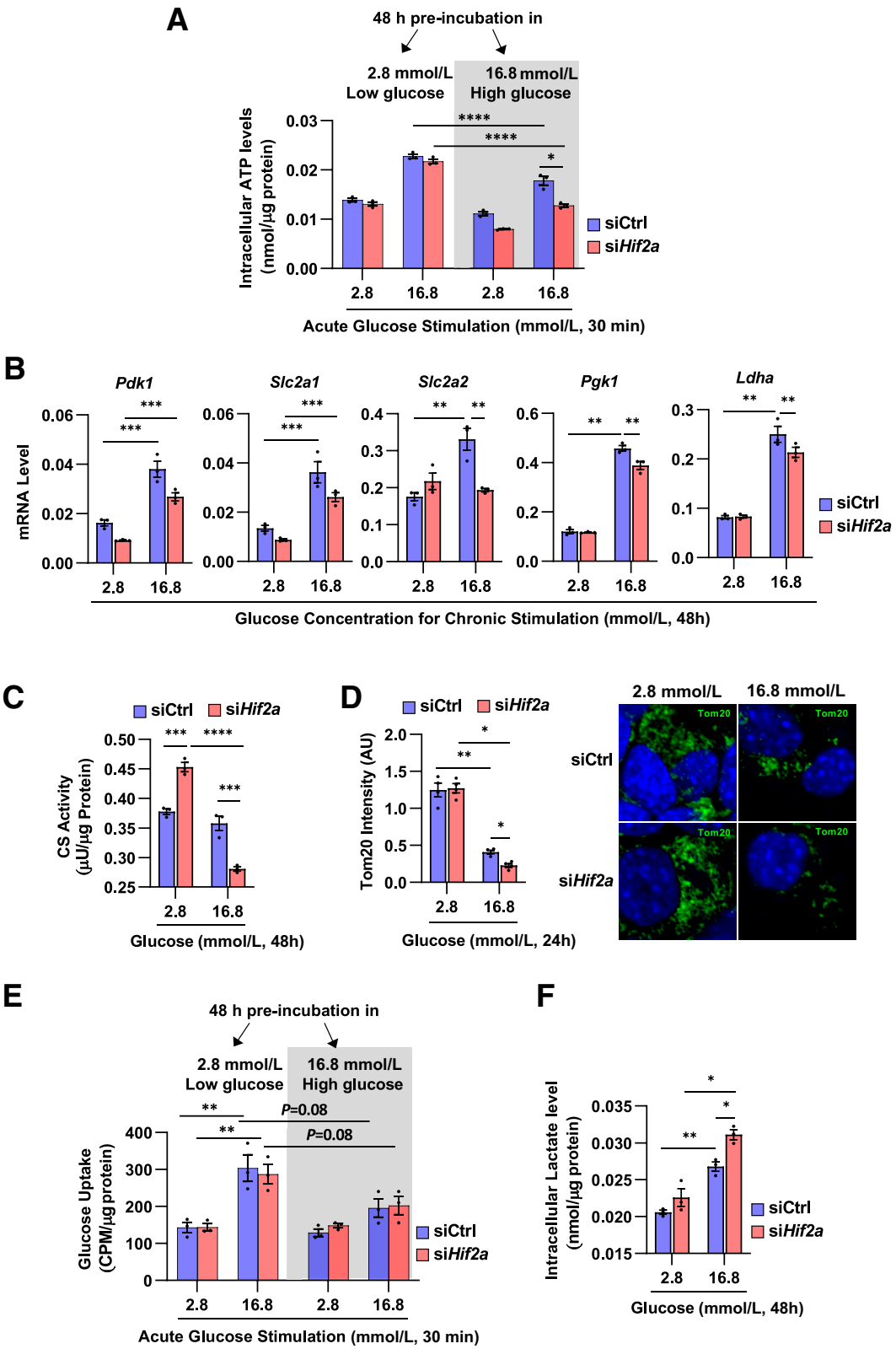

Figure 4—HIF-2α KD sensitizes β-cells to chronic high glucose–induced mitochondrial dysfunction in Min6 cells. Min6 cells were transfected with mock or *Hif2a*-specific siRNA; 24 h after transfection, cells were incubated in low- (2.8 mmol/L) or high-glucose (16.8 mmol/L) media for 24 or 48 h before they are subjected to different assays. *A*: Intracellular ATP levels ($n = 3$ wells per group). *B*: mRNA expression of *Pdk1*, *Slc2a1*, *Slc2a2*, *Pgk1*, and *Ldha* ($n = 3$ wells per group). *C*: CS activity ($n = 3$ wells per group). *D*: Mitochondrial density was determined after staining cells with anti-Tom20 antibodies (green) ($n = 3$ wells per group). *E*: Glucose uptake ($n = 3$ wells per group). *F*: Intracellular lactate levels ($n = 3$ wells per group). $^*P < 0.05$, $^{**}P < 0.01$, $^{***}P < 0.001$, $^{****}P < 0.0001$. All data are presented as mean ± SEM. Statistical analysis was performed by two-way ANOVA with Tukey multiple comparison tests. AU, arbitrary unit.

HIF-2α Induces Antioxidant Gene Expression and Preserves Intact Mitochondria in a Chronic High-Glucose Condition

To test whether the decrease in mitochondrial activity by HIF-2α KD is associated with decreased mitochondrial biogenesis, we measured mitochondrial DNA content and the expression of genes involved in mitochondrial biogenesis. As seen in Fig. 5*A*, mitochondrial DNA content was not changed by HIF-2α KD in Min6 cells incubated in high-glucose media. Moreover, mRNA expression of *Pgc1a*, *Tfam*, *Nrf1*, and *Nrf2*, which are involved in mitochondrial biogenesis, was not decreased by HIF-2α KD (Fig. 5*B*). Therefore, we turned our attention to mitochondrial damage as a possible cause of decreased mitochondrial activity in HIF-2α KD cells. Incubation of mock-transfected control Min6 cells for 24 or 48 h in high-glucose media increased mitochondrial and cytosolic hydrogen peroxide levels (Fig. 5*C* and *D* and Supplementary Fig. 4*E* and *F*). Of interest, HIF-2α KD exaggerated the chronic high glucose–induced ROS levels (Fig. 5*C* and *D* and Supplementary Fig. 4*E* and *F*). Treatment with a mitochondria-specific ROS scavenger, MitoTEMPO, abolished the effect of chronic high glucose to decrease mitochondrial mass (CS activity and Tom20 intensity) in both control and HIF-2α KD cells and, consequently, erased the effect of HIF-2α KD (Fig. 5*E* and *F* and Supplementary Fig. 4*G*). In contrast to the effect of HIF-2α KD, HIF-1α KD decreased ROS levels in Min6 cells incubated in high-glucose media (Supplementary Fig. 4*H*). Overexpression of both HIF-1α and HIF-2α by treatment with a pan PHD inhibitor (64) enhanced high glucose–induced ROS levels, and this effect was completely reversed by HIF-1α KD (Supplementary Fig. 4*H*), suggesting that, opposite to HIF-2α, HIF-1α increases ROS levels. Interestingly, selective induction of HIF-2α with PHD inhibitor treatment in HIF-1α KD cells reduced high glucose–induced ROS levels compared with untreated mock siRNA control or HIF-2α KD cells (Supplementary Fig. 4*H*, lane 3 vs. 4). Together, these results suggest that high glucose–induced HIF-2α, but not HIF-1α, preserves mitochondrial activity by reducing oxidative stress and subsequent mitochondrial damage.

To understand the mechanism through which HIF-2α reduces oxidative stress, we measured pro- and antioxidant gene expression in HIF-2α KD and control cells. Of interest, HIF-2α KD decreased chronic high glucose–induced *Sod2* expression, which encodes mitochondrial antioxidant Mn-SOD (Fig. 5*G*). Moreover, HIF-2α KD decreased *Cat* expression (Fig. 5*G*), which encodes catalase that detoxifies hydrogen peroxide into water. Furthermore, protein levels of SOD2 and catalase were markedly increased after chronic incubation in high-glucose media in an HIF-2α–dependent manner (Fig. 5*H*). Of interest, treatment with MitoTEMPO blocked high glucose–induced SOD2 and catalase expression, along with decreased HIF-2α, suggesting that high glucose–induced antioxidant gene expression is mediated by ROS-dependent HIF-2α expression. Consistent with these results, DNA sequence motif analyses revealed that *SOD2* and *CAT* gene promoters contain putative hypoxia-response elements in both humans and mice (Supplementary Fig. 5). In contrast, the expression of pro-oxidant genes such as *Nox2*, *Nox4*, and $p47^{phox}$, which encode components of NADPH oxidase, were not increased by HIF-2α KD (Fig. 5*I*). *Nos2* (encoding iNOS) expression was slightly increased by HIF-2α KD, but this was accompanied by a decrease in in the expression of *Arg1* (Fig. 5*I*). Arginase competes with iNOS for arginine utilization and functionally suppresses iNOS activity. However, nitric oxide levels were not increased by HIF-2α KD (Fig. 5*J*). Together, these results suggest that HIF-2α suppresses the increase in ROS levels in β-cells after chronic exposure to high glucose levels by stimulating antioxidant gene expression, including *Sod2* and *Cat*.

β-Cell HIF-2α Depletion Enhances Obesity-Induced Oxidative Stress and Mitochondrial Loss in Obese β-Cells

Our results suggest that metabolic stress–induced β-cell HIF-2α preserves mitochondrial activity and GSIS by inducing antioxidant gene expression and decreasing mitochondrial damage. To test this concept in the in vivo setting, we measured ROS levels and intact mitochondrial mass in the islets isolated from HFD-fed H2βKO and WT control mice. As seen in Fig. 6*A* and *B*, ROS levels were increased with decreased intact mitochondrial mass (as measured by CS activity) in the islets from HFD-fed $H2\beta KO^{MIP}$ and $H2\beta KO^{PDX1}$ mice compared with HFD-fed $Cre^{-/-}$:$Hif2a^{fl/fl}$ and MIP-CreERT mice. Moreover, mRNA expression of *Sod2* and *Cat* was significantly decreased in the islets from HFD-fed $H2\beta KO^{MIP}$ mice compared with HFD-fed $Cre^{-/-}$:$Hif2a^{fl/fl}$ mice (Fig. 6*C*). Consistent with this, ex vivo incubation of WT islets in a low-oxygen condition (1%) markedly increased SOD2 and catalase protein expression, and this effect was substantially attenuated in HIF-2α KO islets (Fig. 6*D*). In contrast, mRNA expression of glycolytic genes such as *Pdk1* and *Slc2a1* was not decreased in HIF-2α KO islets (Fig. 6*C*), consistent with the results in Min6 cells chronically incubated in high-glucose media. Taken together, these results suggest that inducible β-cell HIF-2α depletion exacerbates obesity-induced β-cell dysfunction by enhancing oxidative stress and mitochondrial damage in mice (Supplementary Fig. 6).

DISCUSSION

Here, we show that obesity-induced β-cell HIF-2α stimulates antioxidant gene expression and protects against increased oxidative stress and the development of β-cell dysfunction. Metabolic stress induced by chronic incubation of Min6 cells in high-glucose media or by treatment with PA increased HIF-2α expression. HIF-2α KD in Min6 cells exacerbated the chronic high glucose–induced decrease in intracellular ATP levels and GSIS without affecting glucose uptake, whereas it did not affect GSIS in cells maintained in low-glucose media. The decrease in

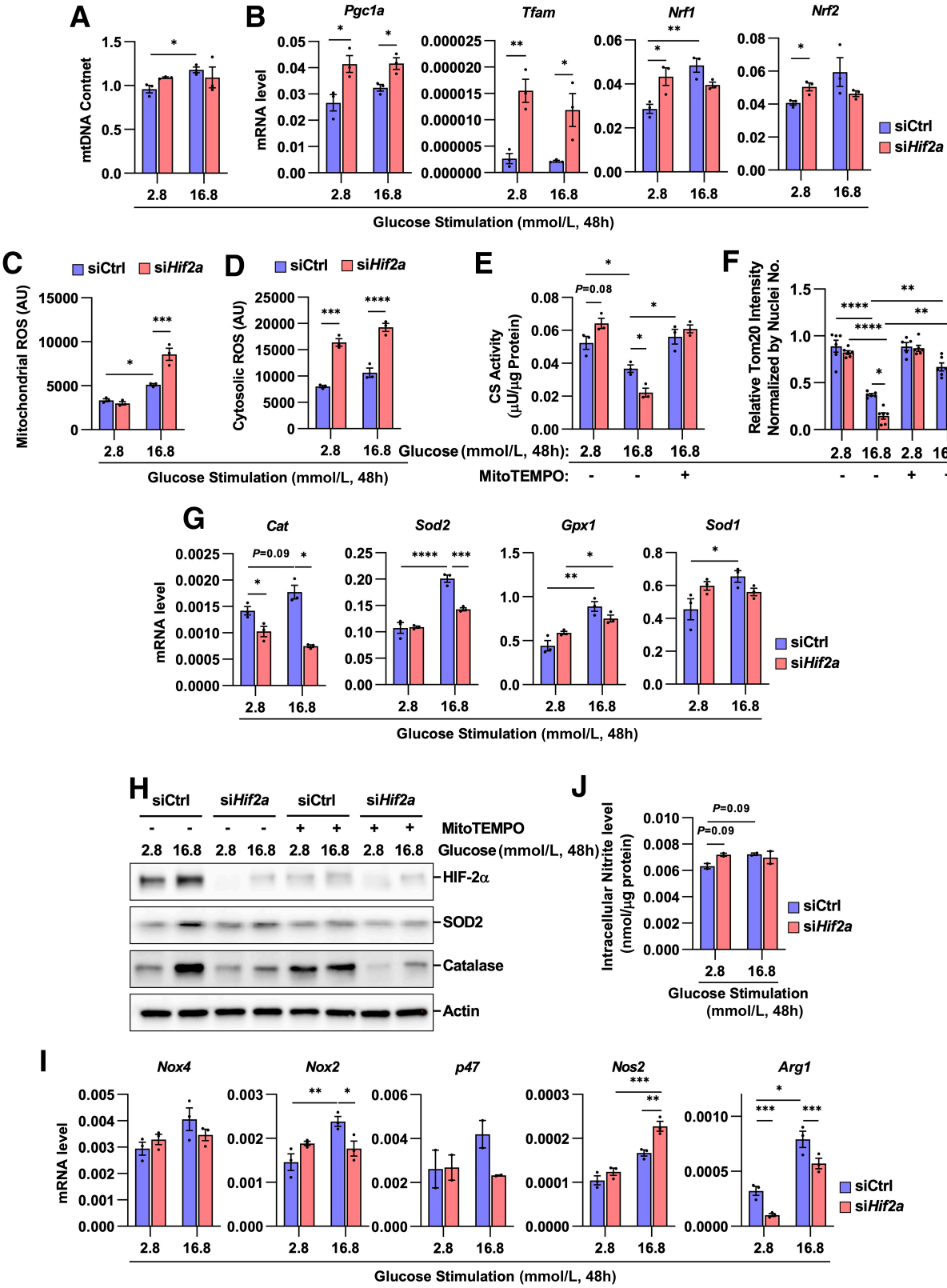

Figure 5—HIF-2α preserves mitochondrial activity in a chronic high-glucose condition by stimulating antioxidant gene expression and reducing oxidative stress in Min6 cells. Min6 cells were transfected with mock or *Hif2a*-specific siRNA; 24 h after transfection, cells were incubated in low- (2.8 mmol/L) or high-glucose (16.8 mmol/L) media for 48 h in the presence or absence of MitoTEMPO. *A*: mtDNA content ($n = 3$ wells per group). *B*: mRNA expression of genes associated with mitochondrial biogenesis ($n = 3$ wells per group). *C*: Mitochondrial ROS levels ($n = 3$ wells per group). *D*: Cytosolic ROS levels ($n = 3$ wells per group). *E*: CS activity. *F*: Mitochondrial density determined by relative Tom20-positive area ($n = 6$ wells per group). *G*: mRNA expression of antioxidant genes ($n = 3$ wells per group). *H*: Western blot

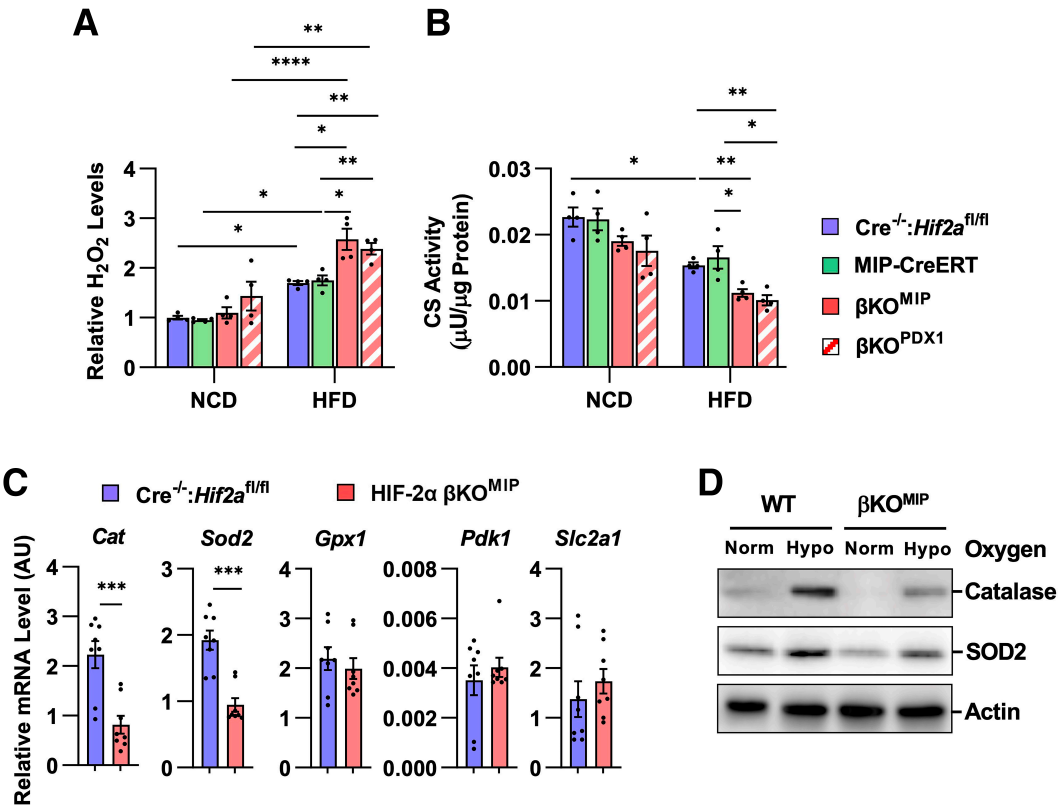

Figure 6—Inducible depletion of β-cell HIF-2α exacerbates HFD-induced islet oxidative stress and β-cell dysfunction. H2βKO^{MIP}, H2βKO^{PDX1}, Cre$^{-/-}$:*Hif2a*$^{fl/fl}$ littermate control, and age-matched MIP-CreERT mice were fed 60% HFD for 12 weeks, followed by 1 week of tamoxifen-containing HFD. After 3 weeks of recovery, mice were euthanized to isolate islets. *A*: Hydrogen peroxide levels in isolated islets ($n = 4$ mice per group). *B*: CS activity in isolated in islets ($n = 4$ mice per group). *C*: mRNA expression of antioxidant and β-cell genes in isolated islets ($n = 8$ mice per group). *D*: Western blot analysis of SOD2 and catalase expression in primary islets from NCD-fed βKO^{MIP} and WT control mice. After isolation, islets were incubated in 37°C normoxic incubator for 24 h for recovery. To induce HIF-2α expression, islets were incubated in hypoxic (1% oxygen) or normoxic chamber for 6 h before undergoing Western blot analysis. *$P < 0.05$, **$P < 0.01$, ***$P < 0.001$, ****$P < 0.001$. All data are presented as mean ± SEM. Statistical analysis was performed by unpaired *t* test (*C*) or two-way ANOVA with Tukey multiple comparison tests (*A* and *B*). Hypo, hypoxia (1% oxygen); Norm, normoxia (21% oxygen).

intracellular ATP levels was due to increased oxidative stress and mitochondrial damage. Treatment with a mitochondria-specific ROS scavenger erased the detrimental effects of HIF-2α KD. At the molecular level, HIF-2α KD reduced the expression of ROS-detoxifying enzymes (e.g., *Sod2* and *Cat*) and enhanced chronic high glucose–induced mitochondrial damage. Consistent with these results, HIF-2α expression was increased in the β-cells of HFD-fed/obese mice compared with NCD-fed/lean mice. Moreover, inducible depletion of β-cell–specific HIF-2α in HFD-fed/obese mice exacerbated β-cell dysfunction and glucose intolerance, with decreased *Sod2* and *Cat* expression, increased ROS levels, and decreased intact mitochondrial mass in the islets. In NCD-fed/lean mice, depletion of HIF-2α did not affect plasma insulin levels or glucose tolerance. Taken together, our results suggest that chronic high glucose–induced β-cell HIF-2α– and HIF-2α–dependent antioxidant enzyme expression constitutes a previously unknown mechanism, allowing β-cells to defend against increased oxidative stress to preserve mitochondrial activity and GSIS in obesity.

Although the mechanism through which obesity induces β-cell dysfunction is relatively well studied, our understanding of how β-cells endure metabolic stress during the development of insulin resistance is limited. Notably, although both β-cell mass and function (GSIS) are decreased in patients with T2DM (5–8), GSIS is greater in the islets from obese individuals without diabetes compared with healthy individuals, and obese individuals without diabetes exhibit relatively normal meal- or glucose-induced plasma insulin levels (65–68). Moreover, individuals with insulin resistance without obesity or diabetes show increased β-cell mass, with

analysis of SOD2 and catalase expression; *I*: mRNA expression of pro-oxidant gene expression ($n = 3$ wells per group). *J*: Intracellular nitrite levels ($n = 2$ wells per group). *$P < 0.05$, **$P < 0.01$, ***$P < 0.001$, ****$P < 0.0001$. All data are presented as mean ± SEM. Statistical analysis was performed by two-way ANOVA with Tukey multiple comparison tests. AU, arbitrary unit.

a trend toward higher in vivo GSIS compared with individuals with insulin sensitivity without obesity or diabetes (69). Similarly, before the onset of hyperglycemia, Zucker fatty rats (at the age of 10–12 weeks) show hypersulinemic normoglycemia with increased in vivo and ex vivo islet GSIS and increased islet mitochondrial glucose metabolism compared with Zucker lean rats (70). This paradoxic increase in β-cell function, even in the presence of increased metabolic stress, suggests that β-cells possess a defense mechanism against metabolic stress early in the development of insulin resistance, which may decline or become insufficient in the later stages of disease.

One of the best-known mechanisms by which metabolic stress induces β-cell dysfunction is through increasing oxidative stress and mitochondrial dysfunction (20). Although β-cells have highly active mitochondrial metabolism, they express relatively low levels of antioxidant enzymes (encoded by genes such as *Sod1*, *Sod2*, *Cat*, and *Gpx1*) compared with liver or kidney (36,37). Therefore, it was suggested that β-cells are vulnerable to chronic oxidative stress. Indeed, several lines of evidence indicates that, although expressed at low levels in the basal state, antioxidant enzymes are necessary to maintain normal β-cell function. Thus, global deletion of *Sod1*, *Sod2*, or *Gpx1* or β-cell–specific deletion of *Fxn* increases oxidative stress in pancreatic islets and causes β-cell dysfunction in mice (71–73). Interestingly, the expression of antioxidant genes such as *Cat*, *Sod2*, and *Gpx1* is increased in the islets of obese mice compared with lean mice (74,75). However, the mechanism through which obesity increases antioxidant gene expression was unknown. Our results suggest that HIF-2α mediates the obesity-induced increase in antioxidant gene expression in β-cells. Because suppression of mitochondrial ROS by MitoTEMPO treatment substantially attenuated high glucose–induced SOD2 and catalase expression, along with decreased HIF-2α, it is likely that ROS-induced HIF-2α expression constitutes a negative feedback mechanism to protect β-cells under metabolic stress. Consistent with our results, it was shown that HIF-2α regulates antioxidant gene expression in liver (76,77). That study showed HIF-2α overexpression drives a seven- to eightfold induction of isolated mouse *Sod2* (approximately −1,452 to +40 bp) and *Cat* (approximately −746 to +76 bp) promoter activity. Consistent with this, we found *SOD2* and *CAT* gene promoters contain putative hypoxia-response elements in both humans and mice. Similar to the phenotypes of β-cell–specific HIF-2α KO mice, *Sod2* heterozygous mice exhibit normal metabolic profile on NCD, but on HFD, these mice develop more severe glucose intolerance compared with WT mice as a result of decreased β-cell GSIS, without changes in insulin sensitivity (72). On the onset of T2DM in humans, islet *SOD2* expression is decreased, whereas *CAT* and *GPx* expression is still increased in the islets from individuals with T2DM compared with healthy individuals (78). Future studies are required to elucidate when and how HIF-2α–dependent induction of antioxidant enzyme expression is compromised during the development of β-cell dysfunction in T2DM.

It is interesting to note that HIF-2α expression was only induced after chronic, but not acute, high-glucose challenge, whereas HIF-1α displayed increased expression after both acute and chronic high-glucose challenges. This raises the possibility that HIF-1α and HIF-2α play distinct roles in response to metabolic stress in β-cells. β-Cell HIF-1α stimulates glycolytic gene expression (e.g., *Slc2a1* or *Pdk1*) required for immediate adaptation to oxygen deprivation (i.e., anaerobic respiration) (79). However, prolonged activation of this can compromise β-cell glucose sensing. Therefore, it is reasonable to hypothesize that HIF-1α mediates immediate responses to increased blood glucose levels. In line with this hypothesis, β-cell–specific HIF-1α KO mice develop β-cell dysfunction and glucose intolerance on NCD (52), whereas overexpression of β-cell HIF-1α by β-cell–specific VHL KO also leads to β-cell dysfunction (80,81). In contrast, we found that HIF-2α KO or KD did not or only marginally affected glycolytic gene expression (e.g., *Slc2a1*, *Ldha*, *Pgk1*, or *Pdk1*) in islets or Min6 cells. Consistently, glucose uptake was unchanged, and intracellular levels of a glycolytic metabolism product, lactate, were increased, but not decreased, by HIF-2α KD. These changes occurred without an increase in HIF-1α expression or activity. Therefore, it is likely that HIF-2α is dispensable for the metabolic switching upon acute high-glucose challenge in normal β-cells. Consistent with this idea, we found HIF-2α KD did not affect GSIS in Min6 cells maintained in low-glucose media. Moreover, β-cell–specific HIF-2α KO mice showed normal glucose tolerance on NCD. However, β-cell HIF-2α KO or KD affected β-cell function in obese mice and in Min6 cells after chronic incubation in high-glucose media. Therefore, we suggest that HIF-2α mediates a delayed response to metabolic stress to protect β-cells from increased oxidative stress. Notably, the glucose-induced acute rise in ROS levels is necessary for full GSIS in normal β-cells by acting as a signaling mediator (15,16). Therefore, it is likely that the HIF-2α–dependent induction of antioxidant enzyme expression is only protective against chronic metabolic stress and does not interfere with acute glucose-induced ROS levels or GSIS in normal β-cells.

Although HIF-1α and HIF-2α share similarities in protein structure, DNA-binding sequence specificity, and regulatory mechanisms (involving VHL and PHDs), several lines of evidence indicate that they mediate distinct metabolic functions. For example, HIF-1α expression is increased in the liver of obese mice (9), whereas postprandial/physiologic increases in liver HIF-2α expression are blunted in obesity (64,82). Obesity-induced hepatocyte HIF-1α enhances first-pass GLP-1 degradation and contributes to the development of glucose intolerance by inducing *Dpp4* expression and sinusoidal flow resistance (9). In contrast, postprandial induction of hepatocyte HIF-

2α suppresses glucagon signaling and increases insulin sensitivity by inducing cAMP-specific phosphodiesterase and *Irs2* expression (64,82,83). In adipocytes, obesity-induced HIF-1α expression stimulates iNOS and expression of various chemokines, triggering adipose tissue inflammation and insulin resistance (55), whereas HIF-2α stimulates UCP1 expression (84) and suppresses weight gain, adipose tissue inflammation, and insulin resistance in HFD-fed/obese mice (55). Our current results suggest that β-cell HIF-2α also plays a protective role against the development of hyperglycemia in obese mice by preserving mitochondrial activity and glucose sensing. Therefore, it seems reasonable to consider a more generalized concept that HIF-2α plays protective roles against the development of hyperglycemia through systemic effects.

Finally, although there are several transgenic mouse strains expressing Cre in β-cells, several problems were raised in all of these mice when we started this study. Thus, most β-cell Cre mice (including the popular rat insulin promoter–Cre and *Pdx*1-Cre mice) show Cre activity in the brain, as well as in β-cells (85). Although mouse insulin promoter–Cre mice show limited Cre expression/activity in adult β-cells, these mice show abnormally increased β-cell size resulting from aberrant expression of a human growth hormone minigene introduced as a part of the DNA-targeting cassette (57,86,87). Therefore, to avoid possible artifacts generated from off-target effects, in the current study, we generated two different inducible β-cell HIF-2α KO mice using MIP-CreERT and *Pdx1*-CreERT mice and tried to extract common phenotypes. Interestingly, $H2\beta KO^{MIP}$ and $H2\beta KO^{PDX1}$ mice exhibited similar metabolic phenotypes, such as exaggeration of HFD-induced islet oxidative stress and mitochondrial dysfunction, leading to impaired GSIS and glucose tolerance. These changes were not associated with changes in β-cell mass or the ratio of α-cells/β-cells on HFD in either KO mouse strain. The only discrepancies we observed between βKO^{MIP} and βKO^{PDX1} mice were the differences in β-cell mass on chow diet. Because the hGH minigene expression in MIP-Cre^{ERT} mice causes β-cell hypertrophy (57), which is absent in βKO^{PDX1} mice, we speculate increased β-cell mass in βKO^{MIP} mice could have been due to combinatorial effects of ectopic hGH minigene expression and the depletion of HIF-2α. Consistent with this idea, we did not find any noticeable changes in cell proliferation or growth after HIF-2α KD in Min6 cells, although we did not directly assess cell death. In addition to this, because HIF-2α protects against oxidative stress, and the islet isolation procedure inevitably causes cellular stress, an additional caveat should be taken into consideration; cellular stress caused during islet isolation could have exaggerated the effect of HIF-2α KO.

In summary, we demonstrate that metabolic stress–induced HIF-2α– and HIF-2α–dependent antioxidant gene expression represent a previously unknown defense mechanism against metabolic stress–induced β-cell dysfunction. Additional studies are necessary to understand whether HIF-2α expression or activity is associated with metabolic health in individuals with obesity and when and how this protective mechanism fails during the course of disease progression, leading to β-cell failure.

Acknowledgments. The authors thank the staff of the San Diego Digestive Disease Research Center and the staff of the La Jolla Institute Microscopy and Histology Core Laboratory for their expert assistance with immunofluorescence staining and slide scanning.

Funding. This study was supported by grant DK124298 from the National Institute of Diabetes and Digestive and Kidney Diseases of the National Institutes of Health (NIH) and University of California San Diego Health Sciences Research Grant RG084153. M.R. was supported by a postdoctoral fellowship from the American Heart Association (16POST29990015). V.H.-A. was supported by grants FPU16/06190 and EST18/00847 from the Ministrio de Educacion, Cultura Deported of Spain. This publication includes data generated or processed at the University of California San Diego Core Laboratories and Centers funded by the NIH (Microscopy Core Laboratory [NS047101] and Histology Core Laboratories [P30CA23100 and P30DK120515]).

Duality of Interest. This study was funded by grants from the Janssen Pharmaceuticals, Inc., Cymabay Therapeutics, Inc., and pH Pharma, LTD. No other potential conflicts of interest relevant to this article were reported.

Author Contributions. J.-S.M. designed and performed a majority of in vitro experiments and histology and mouse tissue analyses and analyzed the data. M.R. performed primary islet isolation and supported mouse experiments. J.B.S., V.H.-A., and R.I. performed in vitro experiments and tissue analysis. Y.S.L. conceived, designed, and supervised the project, interpreted data, and wrote the manuscript. All authors discussed the results and commented on the manuscript. Y.S.L. is the guarantor of this work and, as such, had full access to all the data in the study and takes responsibility for the integrity of the data and the accuracy of the data analysis.

References

1. Halban PA, Polonsky KS, Bowden DW, et al. β-cell failure in type 2 diabetes: postulated mechanisms and prospects for prevention and treatment. Diabetes Care 2014;37:1751–1758

2. Brunzell JD, Robertson RP, Lerner RL, et al. Relationships between fasting plasma glucose levels and insulin secretion during intravenous glucose tolerance tests. J Clin Endocrinol Metab 1976;42:222–229

3. Cavaghan MK, Ehrmann DA, Polonsky KS. Interactions between insulin resistance and insulin secretion in the development of glucose intolerance. J Clin Invest 2000;106:329–333

4. Ferrannini E, Gastaldelli A, Miyazaki Y, Matsuda M, Mari A, DeFronzo RA. Beta-cell function in subjects spanning the range from normal glucose tolerance to overt diabetes: a new analysis. J Clin Endocrinol Metab 2005; 90:493–500

5. Petrenko V, Gandasi NR, Sage D, Tengholm A, Barg S, Dibner C. In pancreatic islets from type 2 diabetes patients, the dampened circadian oscillators lead to reduced insulin and glucagon exocytosis. Proc Natl Acad Sci USA 2020;117:2484–2495

6. Butcher MJ, Hallinger D, Garcia E, et al. Association of proinflammatory cytokines and islet resident leucocytes with islet dysfunction in type 2 diabetes. Diabetologia 2014;57:491–501

7. Butler AE, Janson J, Bonner-Weir S, Ritzel R, Rizza RA, Butler PC. Beta-cell deficit and increased beta-cell apoptosis in humans with type 2 diabetes. Diabetes 2003;52:102–110

8. Polonsky KS. Dynamics of insulin secretion in obesity and diabetes. Int J Obes Relat Metab Disord 2000;24(Suppl. 2):S29–S31

9. Lee YS, Riopel M, Cabrales P, Bandyopadhyay GK. Hepatocyte-specific HIF-1α ablation improves obesity-induced glucose intolerance by reducing first-pass GLP-1 degradation. Sci Adv 2019;5:eaaw4176
10. Vilsbøll T, Krarup T, Deacon CF, Madsbad S, Holst JJ. Reduced postprandial concentrations of intact biologically active glucagon-like peptide 1 in type 2 diabetic patients. Diabetes 2001;50:609–613
11. Hudish LI, Reusch JE, Sussel L. β cell dysfunction during progression of metabolic syndrome to type 2 diabetes. J Clin Invest 2019;129:4001–4008
12. Talchai C, Lin HV, Kitamura T, Accili D. Genetic and biochemical pathways of beta-cell failure in type 2 diabetes. Diabetes Obes Metab 2009;11(Suppl. 4):38–45
13. Cadenas E, Davies KJA. Mitochondrial free radical generation, oxidative stress, and aging. Free Radic Biol Med 2000;29:222–230
14. Neal A, Rountree A, Kernan K, et al. Real-time imaging of intracellular hydrogen peroxide in pancreatic islets. Biochem J 2016;473:4443–4456
15. Leloup C, Tourrel-Cuzin C, Magnan C, et al. Mitochondrial reactive oxygen species are obligatory signals for glucose-induced insulin secretion. Diabetes 2009;58:673–681
16. Pi J, Bai Y, Zhang Q, et al. Reactive oxygen species as a signal in glucose-stimulated insulin secretion. Diabetes 2007;56:1783–1791
17. Haythorne E, Rohm M, van de Bunt M, et al. Diabetes causes marked inhibition of mitochondrial metabolism in pancreatic β-cells. Nat Commun 2019;10:2474
18. Fex M, Nicholas LM, Vishnu N, et al. The pathogenetic role of β-cell mitochondria in type 2 diabetes. J Endocrinol 2018;236:R145–R159
19. Silva JP, Köhler M, Graff C, et al. Impaired insulin secretion and beta-cell loss in tissue-specific knockout mice with mitochondrial diabetes. Nat Genet 2000;26:336–340
20. Lu H, Koshkin V, Allister EM, Gyulkhandanyan AV, Wheeler MB. Molecular and metabolic evidence for mitochondrial defects associated with beta-cell dysfunction in a mouse model of type 2 diabetes. Diabetes 2010;59:448–459
21. Maassen JA, 'T Hart LM, Van Essen E, et al. Mitochondrial diabetes: molecular mechanisms and clinical presentation. Diabetes 2004;53(Suppl. 1):S103–S109
22. Back SH, Scheuner D, Han J, et al. Translation attenuation through eIF2α phosphorylation prevents oxidative stress and maintains the differentiated state in β cells. Cell Metab 2009;10:13–26
23. Marchetti P, Bugliani M, Lupi R, et al. The endoplasmic reticulum in pancreatic beta cells of type 2 diabetes patients. Diabetologia 2007;50:2486–2494
24. Porte D Jr, Kahn SE. beta-cell dysfunction and failure in type 2 diabetes: potential mechanisms. Diabetes 2001;50(Suppl. 1):S160–S163
25. Ying W, Lee YS, Dong Y, et al. Expansion of islet-resident macrophages leads to inflammation affecting β cell proliferation and function in obesity. Cell Metab 2019;29:457–474.e5
26. Newsholme P, Keane KN, Carlessi R, Cruzat V. Oxidative stress pathways in pancreatic β-cells and insulin-sensitive cells and tissues: importance to cell metabolism, function, and dysfunction. Am J Physiol Cell Physiol 2019;317:C420–C433
27. Muhammed SJ, Lundquist I, Salehi A. Pancreatic β-cell dysfunction, expression of iNOS and the effect of phosphodiesterase inhibitors in human pancreatic islets of type 2 diabetes. Diabetes Obes Metab 2012;14:1010–1019
28. Nakayama M, Inoguchi T, Sonta T, et al. Increased expression of NAD(P)H oxidase in islets of animal models of type 2 diabetes and its improvement by an AT1 receptor antagonist. Biochem Biophys Res Commun 2005;332:927–933
29. Bindokas VP, Kuznetsov A, Sreenan S, Polonsky KS, Roe MW, Philipson LH. Visualizing superoxide production in normal and diabetic rat islets of Langerhans. J Biol Chem 2003;278:9796–9801
30. Abebe T, Mahadevan J, Bogachus L, et al. Nrf2/antioxidant pathway mediates β cell self-repair after damage by high-fat diet-induced oxidative stress. JCI Insight 2017;2:e92854
31. Anello M, Lupi R, Spampinato D, et al. Functional and morphological alterations of mitochondria in pancreatic beta cells from type 2 diabetic patients. Diabetologia 2005;48:282–289
32. Del Guerra S, Lupi R, Marselli L, et al. Functional and molecular defects of pancreatic islets in human type 2 diabetes. Diabetes 2005;54:727–735
33. Kaneto H, Kajimoto Y, Miyagawa J, et al. Beneficial effects of antioxidants in diabetes: possible protection of pancreatic beta-cells against glucose toxicity. Diabetes 1999;48:2398–2406
34. Tajiri Y, Möller C, Grill V. Long-term effects of aminoguanidine on insulin release and biosynthesis: evidence that the formation of advanced glycosylation end products inhibits B cell function. Endocrinology 1997;138:273–280
35. Ighodaro OM, Akinloye OA. First line defence antioxidants-superoxide dismutase (SOD), catalase (CAT) and glutathione peroxidase (GPX): Their fundamental role in the entire antioxidant defence grid. Alex J Med 2019;54:287–293
36. Lenzen S, Drinkgern J, Tiedge M. Low antioxidant enzyme gene expression in pancreatic islets compared with various other mouse tissues. Free Radic Biol Med 1996;20:463–466
37. Sigfrid LA, Cunningham JM, Beeharry N, et al. Antioxidant enzyme activity and mRNA expression in the islets of Langerhans from the BB/S rat model of type 1 diabetes and an insulin-producing cell line. J Mol Med (Berl) 2004;82:325–335
38. Harmon JS, Bogdani M, Parazzoli SD, et al. Beta-cell-specific overexpression of glutathione peroxidase preserves intranuclear MafA and reverses diabetes in db/db mice. Endocrinology 2009;150:4855–4862
39. Bertera S, Crawford ML, Alexander AM, et al. Gene transfer of manganese superoxide dismutase extends islet graft function in a mouse model of autoimmune diabetes. Diabetes 2003;52:387–393
40. Xu B, Moritz JT, Epstein PN. Overexpression of catalase provides partial protection to transgenic mouse beta cells. Free Radic Biol Med 1999;27:830–837
41. Kubisch HM, Wang J, Bray TM, Phillips JP. Targeted overexpression of Cu/Zn superoxide dismutase protects pancreatic beta-cells against oxidative stress. Diabetes 1997;46:1563–1566
42. Chen H, Li X, Epstein PN. MnSOD and catalase transgenes demonstrate that protection of islets from oxidative stress does not alter cytokine toxicity. Diabetes 2005;54:1437–1446
43. Ivan M, Kaelin WG Jr. The EGLN-HIF O_2-sensing system: multiple inputs and feedbacks. Mol Cell 2017;66:772–779
44. Schödel J, Ratcliffe PJ. Mechanisms of hypoxia signalling: new implications for nephrology. Nat Rev Nephrol 2019;15:641–659
45. Semenza GL. Pharmacologic targeting of hypoxia-inducible factors. Annu Rev Pharmacol Toxicol 2019;59:379–403
46. Keith B, Johnson RS, Simon MC. HIF1α and HIF2α: sibling rivalry in hypoxic tumour growth and progression. Nat Rev Cancer 2011;12:9–22
47. Heinis M, Simon MT, Ilc K, et al. Oxygen tension regulates pancreatic beta-cell differentiation through hypoxia-inducible factor 1alpha. Diabetes 2010;59:662–669
48. Chen H, Houshmand G, Mishra S, Fong GH, Gittes GK, Esni F. Impaired pancreatic development in Hif2-alpha deficient mice. Biochem Biophys Res Commun 2010;399:440–445
49. Bensellam M, Duvillié B, Rybachuk G, et al. Glucose-induced O_2 consumption activates hypoxia inducible factors 1 and 2 in rat insulin-secreting pancreatic beta-cells. PLoS One 2012;7:e29807
50. Van de Velde S, Hogan MF, Montminy M. mTOR links incretin signaling to HIF induction in pancreatic beta cells. Proc Natl Acad Sci USA 2011;108:16876–16882
51. Gunton JE, Kulkarni RN, Yim S, et al. Loss of ARNT/HIF1β mediates altered gene expression and pancreatic-islet dysfunction in human type 2 diabetes. Cell 2005;122:337–349
52. Cheng K, Ho K, Stokes R, et al. Hypoxia-inducible factor-1alpha regulates beta cell function in mouse and human islets. J Clin Invest 2010;120:2171–2183
53. Tamarina NA, Roe MW, Philipson L. Characterization of mice expressing Ins1 gene promoter driven CreERT recombinase for conditional gene deletion in pancreatic β-cells. Islets 2014;6:e27685

54. Gu G, Dubauskaite J, Melton DA. Direct evidence for the pancreatic lineage: NGN3+ cells are islet progenitors and are distinct from duct progenitors. Development 2002;129:2447–2457
55. Lee YS, Kim JW, Osborne O, et al. Increased adipocyte O2 consumption triggers HIF-1α, causing inflammation and insulin resistance in obesity. Cell 2014;157:1339–1352
56. Lee YS, Li P, Huh JY, et al. Inflammation is necessary for long-term but not short-term high-fat diet-induced insulin resistance. Diabetes 2011;60:2474–2483
57. Carboneau BA, Le TD, Dunn JC, Gannon M. Unexpected effects of the MIP-CreER transgene and tamoxifen on β-cell growth in C57Bl6/J male mice. Physiol Rep 2016;4:e12863
58. Lee YS, Morinaga H, Kim JJ, et al. The fractalkine/CX3CR1 system regulates β cell function and insulin secretion. Cell 2013;153:413–425
59. Gupta D, Jetton TL, LaRock K, et al. Temporal characterization of β cell-adaptive and -maladaptive mechanisms during chronic high-fat feeding in C57BL/6NTac mice. J Biol Chem 2017;292:12449–12459
60. Lee KY, Gesta S, Boucher J, Wang XL, Kahn CR. The differential role of Hif1β/Arnt and the hypoxic response in adipose function, fibrosis, and inflammation. Cell Metab 2011;14:491–503
61. Nagai Y, Matsuoka TA, Shimo N, et al. Glucotoxicity-induced suppression of Cox6a2 expression provokes β-cell dysfunction via augmented ROS production. Biochem Biophys Res Commun 2021;556:134–141
62. Poitout V, Robertson RP. Glucolipotoxicity: fuel excess and beta-cell dysfunction. Endocr Rev 2008;29:351–366
63. Robertson RP, Zhang HJ, Pyzdrowski KL, Walseth TF. Preservation of insulin mRNA levels and insulin secretion in HIT cells by avoidance of chronic exposure to high glucose concentrations. J Clin Invest 1992;90:320–325
64. Riopel M, Moon J-S, Bandyopadhyay GK, et al. Inhibition of prolyl hydroxylases increases hepatic insulin and decreases glucagon sensitivity by an HIF-2α-dependent mechanism. Mol Metab 2020;41:101039
65. Mezghenna K, Pomiès P, Chalançon A, et al. Increased neuronal nitric oxide synthase dimerisation is involved in rat and human pancreatic beta cell hyperactivity in obesity. Diabetologia 2011;54:2856–2866
66. Brandhorst H, Brandhorst D, Hering BJ, Federlin K, Bretzel RG. Body mass index of pancreatic donors: a decisive factor for human islet isolation. Exp Clin Endocrinol Diabetes 1995;103(Suppl. 2):23–26
67. Polonsky KS, Given BD, Van Cauter E. Twenty-four-hour profiles and pulsatile patterns of insulin secretion in normal and obese subjects. J Clin Invest 1988;81:442–448
68. Polonsky KS, Given BD, Hirsch L, et al. Quantitative study of insulin secretion and clearance in normal and obese subjects. J Clin Invest 1988;81:435–441
69. Mezza T, Muscogiuri G, Sorice GP, et al. Insulin resistance alters islet morphology in nondiabetic humans. Diabetes 2014;63:994–1007
70. Liu YQ, Jetton TL, Leahy JL. Beta-cell adaptation to insulin resistance. Increased pyruvate carboxylase and malate-pyruvate shuttle activity in islets of nondiabetic Zucker fatty rats. J Biol Chem 2002;277:39163–39168
71. Wang X, Vatamaniuk MZ, Roneker CA, et al. Knockouts of SOD1 and GPX1 exert different impacts on murine islet function and pancreatic integrity. Antioxid Redox Signal 2011;14:391–401
72. Kang L, Dai C, Lustig ME, et al. Heterozygous SOD2 deletion impairs glucose-stimulated insulin secretion, but not insulin action, in high-fat-fed mice. Diabetes 2014;63:3699–3710
73. Muscogiuri G, Salmon AB, Aguayo-Mazzucato C, et al. Genetic disruption of SOD1 gene causes glucose intolerance and impairs β-cell function. Diabetes 2013;62:4201–4207
74. Hasnain SZ, Borg DJ, Harcourt BE, et al. Glycemic control in diabetes is restored by therapeutic manipulation of cytokines that regulate beta cell stress. Nat Med 2014;20:1417–1426
75. Chan JY, Luzuriaga J, Bensellam M, Biden TJ, Laybutt DR. Failure of the adaptive unfolded protein response in islets of obese mice is linked with abnormalities in β-cell gene expression and progression to diabetes. Diabetes 2013;62:1557–1568
76. Scortegagna M, Ding K, Oktay Y, et al. Multiple organ pathology, metabolic abnormalities and impaired homeostasis of reactive oxygen species in Epas1-/- mice. Nat Genet 2003;35:331–340
77. Oktay Y, Dioum E, Matsuzaki S, et al. Hypoxia-inducible factor 2α regulates expression of the mitochondrial aconitase chaperone protein frataxin. J Biol Chem 2007;282:11750–11756
78. Marchetti P, Del Guerra S, Marselli L, et al. Pancreatic islets from type 2 diabetic patients have functional defects and increased apoptosis that are ameliorated by metformin. J Clin Endocrinol Metab 2004;89:5535–5541
79. Sato Y, Endo H, Okuyama H, et al. Cellular hypoxia of pancreatic beta-cells due to high levels of oxygen consumption for insulin secretion in vitro. J Biol Chem 2011;286:12524–12532
80. Zehetner J, Danzer C, Collins S, et al. PVHL is a regulator of glucose metabolism and insulin secretion in pancreatic beta cells. Genes Dev 2008;22:3135–3146
81. Cantley J, Selman C, Shukla D, et al. Deletion of the von Hippel-Lindau gene in pancreatic beta cells impairs glucose homeostasis in mice. J Clin Invest 2009;119:125–135
82. Ramakrishnan SK, Zhang H, Takahashi S, et al. HIF2α is an essential molecular brake for postprandial hepatic glucagon response independent of insulin signaling. Cell Metab 2016;23:505–516
83. Taniguchi CM, Finger EC, Krieg AJ, et al. Cross-talk between hypoxia and insulin signaling through Phd3 regulates hepatic glucose and lipid metabolism and ameliorates diabetes. Nat Med 2013;19:1325–1330
84. García-Martín R, Alexaki VI, Qin N, et al. Adipocyte-specific hypoxia-inducible factor 2α deficiency exacerbates obesity-induced brown adipose tissue dysfunction and metabolic dysregulation. Mol Cell Biol 2015;36:376–393
85. Magnuson MA, Osipovich AB. Pancreas-specific Cre driver lines and considerations for their prudent use. Cell Metab 2013;18:9–20
86. Oropeza D, Jouvet N, Budry L, et al. Phenotypic characterization of MIP-CreERT1Lphi mice with transgene-driven islet expression of human growth hormone. Diabetes 2015;64:3798–3807
87. Brouwers B, de Faudeur G, Osipovich AB, et al. Impaired islet function in commonly used transgenic mouse lines due to human growth hormone minigene expression. Cell Metab 2014;20:979–990